Proceedings of 12th Cambridge Workshop on Cool Stars, Stellar Systems, & The Sun, 2003 University of Colorado.

Triggered Low Mass Star Formation in the Gum Nebula: CG30/31/38 and CG4/6/SA101

Jinyoung Serena Kim[1], Frederick M. Walter[1], Scott J. Wolk[2]

Abstract. High mass stars can terminate low mass star formation (LMSF), but can also trigger it. The Gum Nebula is an excellent site to study how high mass stars influence LMSF. The nebula contains SNRs, OB stars, and cometary globules (CGs). We present multi-wavelength photometric studies of selected regions in CG30/31/38 and optical photometry on CG4/6/SA101. We identify loci of likely pre-main sequence (PMS) stars as well as near-IR excess sources from their color-magnitude and color-color diagrams. CG4/6/SA101 is near γ^2 Vel and Vela OB2, which may have influenced its LMSF. The X-ray sources around CG30/31/38 outline the heads of the CGs pointing toward central ionizing sources. We find two parallel loci of candidate PMS stars in which older ones may have disks while younger ones ($\leq$2Myr) may not. This region has probably been influenced by ζ Pup and/or the progenitor of Vela SNR.

1. Introduction

From their birth to death high mass stars play an important role in low mass star formation (LMSF). The UV radiation and winds from high mass stars ionize and sweep away low density gas of surrounding clouds preventing condensation of clouds, and strong winds and supernova explosions disrupt their parental cloud. However the pressure induced by radiation and winds can also collapse surrounding clouds starting LMSF in the cores of remnant clouds. A useful site to study triggered LMSF is cometary globules (CGs). CGs are evaporating molecular cloud cores with a head-tail geometry. They are bright-rimmed dark clouds illuminated by UV sources, and are often seen in HII regions near OB stars. The Gum Nebula contains a number of spectacular CGs with signs of LMSF (e.g. Reipurth 1983; Pettersson 1984; Sahu etal. 1988), as well as supernovae remnants (SNRs) and OB associations. The nebula is the largest apparent HII region (Gum 1952) with linear diameter of 250 pc at distance of 450 pc. The nebula might be an old SNR, a fossil Strömgren sphere, and/or a stellar wind bubble. ζ Pup(O4If), γ^2 Vel(WC8+O7.5I), and two OB associations (Tr 10 and Vela OB2) near its morphological center can account for most of photoionization in the nebula. Their radiation driven wind is probably the cause behind evaporation of CGs (Bertoldi and McKee 1990, Lefloch and Lazareff 1994). Here we

[1]Dept. of Physics and Astronomy, State University of New York, Stony Brook, NY 11794-3800, USA

[2]Harvard-Smithsonian Center for Astrophysics, 60 Garden Street, Cambridge, MA 02138, USA

explore two CG complexes around CG30/31/38 and CG4/6/SA101 in the Gum Nebula to study triggered star formation under harsh physical conditions.

2. Observations

2.1. X-ray

Using the ROSAT/HRI (40' diameter) we observed the CG30/31/38 complex, and identified 14 X-ray sources (limiting mag V$\sim$16). These X-ray sources do not show random spatial distribution, but outline the CG heads (Figure 2). X-rays are an excellent means of selecting candidate low mass PMS stars (e.g., Walter et al. 1988), because these stars are generally rapidly rotating and highly convective, the two ingredients which generate solar-like coronal and chromospheric activity.

2.2. Optical

We obtained optical photometry of the X-ray sources using the CTIO/0.9m telescope during Jan 29-30, 1996 and Mar 6-7, 2001. We used U,B,V,R,I filters with 2048×2048 CCD (0.37"/pixel, 13.6'×13.6' FOV). Here we present 2 fields (boxes in Fig 1a) where X-ray sources appear to be concentrated under CG30 and 31. We also present 4 fields in CG4/6/SA101 region (yellow boxes in Fig 1b). All of the fields have long exposures of 60 sec and 300 sec for fields in CG30/31/38 (1996) and in CG4/6/SA101 (2001) respectively, as well as short exposures (20 sec and 10 sec) to avoid saturation of bright stars. We observed several fields of standard stars several times per night. We reduced the images with IRAF/DAOPHOT package. Since the point spread function (PSF) varies depending on the location of the CCD, we selected 40-80 PSF stars in each field, and determined the PSF using quadratic fits in both axes of the CCD. Magnitudes were then corrected to the larger aperture (18 pixels) which was used for the photometry of standard stars. The photometric errors are $\sim$1% at V$\sim$18, and $\sim$5% at V$\sim$21. The aperture correction is good to $\sim 1-2\%$.

2.3. Near-IR

For the CG30/31/38 region, we obtained JHK images using CIRIM detector with CTIO/1.5m telescope near ROSAT/HRI X-ray sources during Feb 5-6, 1996 and Feb 17-20, 1997. CIRIM uses a 256×256 HgCdTe NICMOS 3 array, and we used f/30 (0.″30/pixel,75" FOV). Images were rastered for the median filtering of the sky. We used 6 images for the default raster patterns for an object, and 4 images for a standard star. The data was reduced and analyzed using IDL/DoCIRIM software (Walter, 2000) and custom written IDL softwares. We observed some standard stars in the Elias(CIT, Elias 1982) and FS(UKIRT) standard star lists. We used a 20 pixel radius aperture for standard stars, and 3,5, or 7 pixel radii apertures for the objects, and then applied an aperture correction. The photometric error at K=16 mag varies from few% to 50% depending on the weather conditions as well as on the aperture size we chose. In this study, we used only those with photometric error $\leq$5% (K$\sim$15 mag).

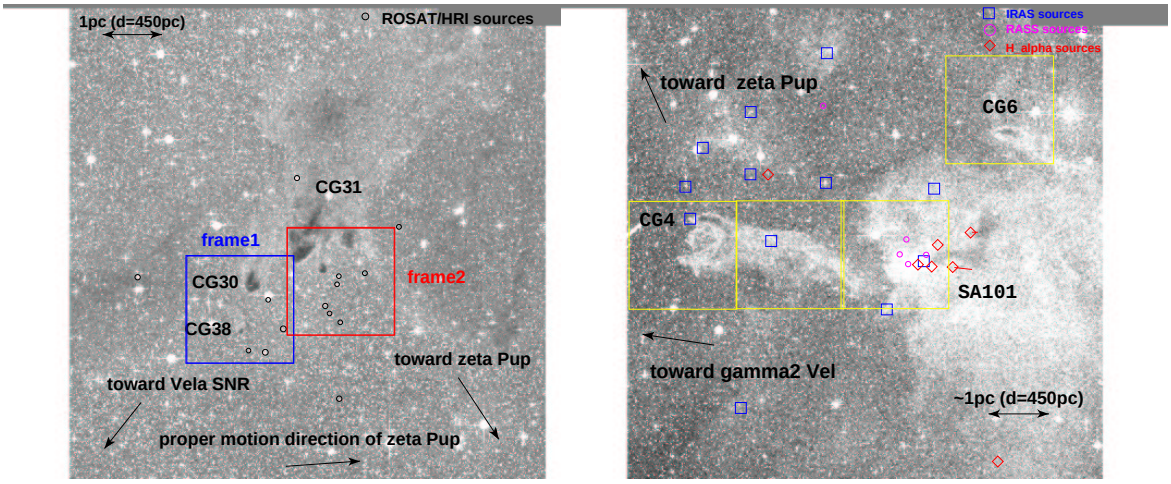

Figure 1. **a (left):** A DSS image (60'×60') of CG30/31/38 complex. ROSAT/HRI X-ray sources are circled. The directions to the central ionizing sources and proper motion of ζ Pup are indicated with arrows. **b (right):** A DSS image (60'×60') of CG4/6/SA101 complex. Sources within the yellow boxes are discussed in this study. Red diamonds are Hα sources, magenta circles are RASS sources, and blue boxes are IRAS sources. Arrows are directions towards γ^2 Vel and ζ Pup.

3. Signs of Low Mass Star Formation

3.1. CG30/31/38

Fig 1a is the digital sky survey (DSS) image of the CG30/31/38 complex. CG30 contains HH 120/IRAS source CG30-IRS4 (Pettersson 1984). The X-ray sources appear to lie between the CG heads and the central ionizing sources. Fig 2a is the V-I vs V CMD of this complex. There are ~180 stars lying along the PMS loci with age ≤30Myr at d=300pc. The termination of the X-ray sources at V~16 represents the limiting X-ray flux f_x. The ratio f_x/f_v of PMS stars is approximately constant from 10^{-3} to 10^{-4} over this color range. The existence of 2 parallel loci in Fig 2a is suggested by the CMD, and is most easily seen by the X-ray data points. This may suggest two distinct episodes of star formation, or two star forming regions at different distances. Stars marked with red crosses lie along the same birthline indicating younger ages than stars marked with blue asterisks if they are at the same distance. Interestingly, all red asterisks are from the frame2 in Fig 1a below CG31, while blue ones are from the frame1 under CG30. X-ray sources in frame2 appear to be more clustered and also have more IR sources than in frame1, but the frame2 sources do not have IR excesses! *Are these signs of more recent formation below CG31 evidence of triggered LMSF by the influence of a runaway supergiant ζ Pup ?*

Note that the direction and morphology of the CG31 tails are consistent with the proper-motion direction of ζ Pup. ζ Pup is an early O type supergiant with T_{eff} ~43000K, has a space velocity of ~ 70-120 km/sec (van Rensbergen et al. 1996), and may have traveled from the direction of Tr 10 or Vela Molecular

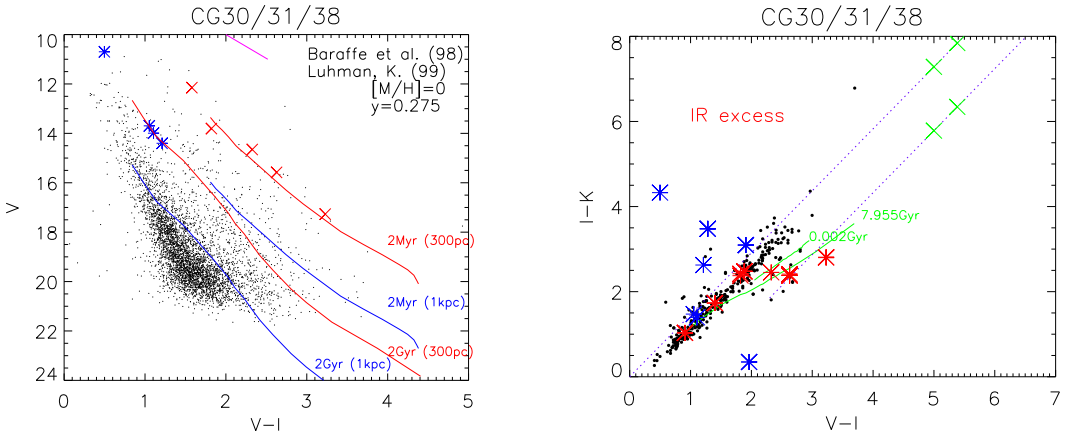

Figure 2. **a (left):** V-I vs V color-magnitude diagram (CMD) of CG30/31/38 complex. Total 4461 stars are plotted. Stars which are likely counterparts of X-ray sources are indicated with crosses and asterisks (blue and red sources from blue and red boxes (frame1 and frame2) in Fig 1a). The reddening vector is the magenta line running almost parallel to the isochrones. The isochrones are from Baraffe et al. (1998), modified using Luhman(1999)'s temperature scale at an assumed distances of 300pc (red line) and 1kpc (blue line). **b (right):** V-I vs I-K diagram of CG30/31/38 region. Asterisks are likely optical/IR counterparts of X-ray sources. Green crosses indicate reddening vectors, solid lines are isochorones for 2Myr and 8Gyr, and the dotted (purple) lines indicate normal photosphere (no disk) and their reddening direction. Note that 4 of the blue asterisks appear in the IR excess region which indicates the possible presence of circumstellar disks.

Ridge to current location. The birth site of ζ Pup is not known, however given the proper motion direction of this star, the change of tail directions of CG31 complex suggest that these clouds are likely influenced by ζ Pup. Fig 2b is the (V-I) vs (I-K) color-color diagram of CG30/31/38 complex. Asterisks are near-IR and optical counterparts within the X-ray error circles (blue* from frame1 and red* from frame2). Why do the blue asterisks (which lie on older locus in CMD) have near-IR excess? They may be 1kpc away while red ones are much nearer, or may be at the same distance while the red ones may be much younger but have lost the disks due to the photoevaporation by UV radiation of ionizing sources.

3.2. CG4/6/SA101

Fig 1b is the DSS image of CG4/6/SA101 region. We present optical photometric study on four fields (yellow boxes). Photometry was done around the CG4, CG6 and SA101 covering Rosat All Sky Survey (RASS), IRAS, and Hα sources (Reipurth and Pettersson 1993). The head of CG4 has been eroded possibly by radiation from γ^2 Vel and OB stars in Vela OB2. CG6 is much smaller than CG4, and is located to the north-west of CG4 and above SA101 cloud. SA101

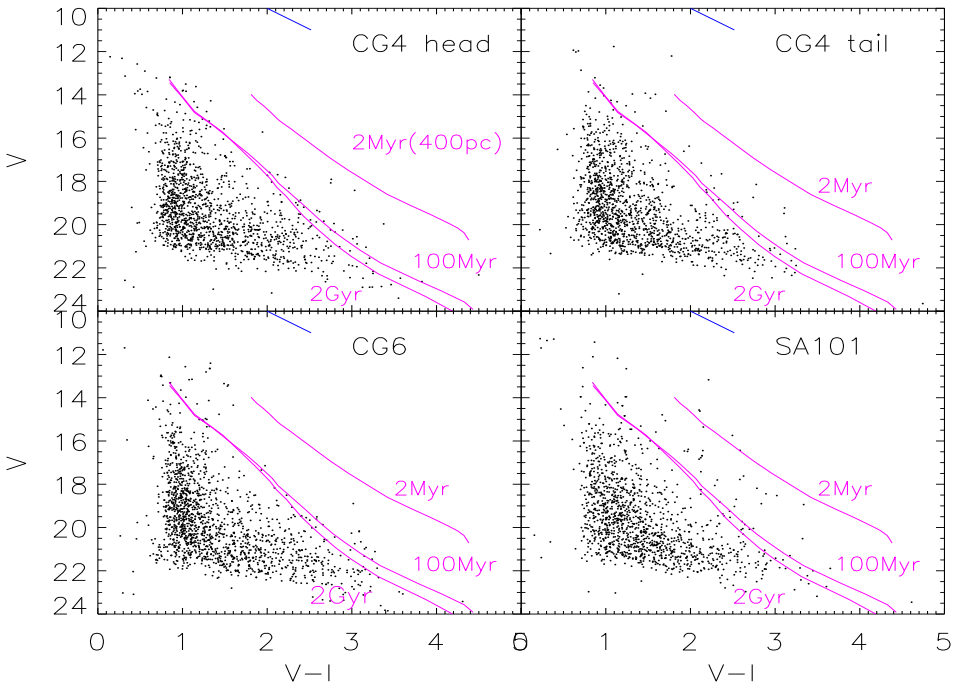

Figure 3. V-I vs V color-magnitude diagram (CMD) of CG4/6/SA101 region. Magenta lines are isochrones at distance 400pc from Baraffe et al. (1998) modified using Luhman's temperature scale (1999) for low mass stars. blue lines on the top of the CMDs are reddening vectors.

is a much larger cloud with Hα sources and RASS sources concentrated on its central part right behind the tail of CG4. While CG4 was exposed to UV radiation, SA101 may have been protected by the once-larger parent cloud of CG4. In Fig 3 we present CMDs of the head and tail of CG4, as well as CG6, and SA101. The head of CG4 show few PMS candidates as does the tail. There are no candidate PMS stars in CG6 region, while SA101 reveals a number of PMS candidates. The isochrones (Baraffe et al. 1998, Luhman 1999) are plotted for a 400pc distance. We find ∼40 stars lying on PMS locus (≤100Myr) for SA101, ∼5-10 for CG4 head, ∼24 for CG4 tail, and none in CG6.

4. Summary

There are indeed candidate PMS stars in the CG30/31/38 and CG4/6/SA101 regions. Here we summarize what we have learned from this study.

CG30/31/38

• The spatial distribution of X-ray sources around these CGs suggest triggered LMSF. We find ∼180 candidate PMS stars (out of 4461 stars) from their loca-

tion in the CMD using the isochrone at 300pc.
• The two parallel loci in Fig 2a may be due to two different episodes of LMSF, or two different distances (200-450pc and ∼1kpc). The morphology of disrupted CG31 tails and heads coincide with the proper motion direction of ζ Pup. This may give more weight on the scenario of the two different episodes of LMSF.
• Younger PMS candidates (red crosses from frame2) do not show IR excesses (disks) while older ones (blue *) do (Fig 2b). The blue data points may be young stars at distance >1kpc still having disks. If they are at the same distance, one possibility is that the UV radiation from O stars (ζ Pup?) selectively photoevaporated some disks at a very early stage of their formation.

CG4/6/SA101

• There are few PMS candidates around CG4, none around CG6, and ∼40 in SA101. Stars on the PMS locus in CG4 seem to be older than in SA101. There are only a few stars on the PMS loci in the CMD of CG4 head. Why is there no star formation activity in the eroded head of CG4? Perhaps there is an age gradient from the CG4 head to tail to the SA101 region. If so, the LMSF in this region might have happened gradually under the influence of high mass stars in Vela OB2, such as γ^2 Vel.
• Is γ^2 Vel the major trigger of LMSF in this region? Perhaps CG4 and CG6 were part of the same cloud as SA101, but evaporated first thus shielding the SA101 cloud which only began LMSF activities more recently. Candidate PMS stars in SA101 may be influenced by γ^2 Vel if they are at ∼400pc, however stars in PMS loci in CG4 may be too old to have been influenced by γ^2 Vel at the same distance.

References

Baraffe, I., Chabrier, G., Allard, F., and Hauschildt, P. H. 1998, A&A **337**, 403.

Bertoldi, F.M.,McKee,C. 1990, ApJ, **354**, 529

Brand, P.W.J.L., Hawarden, T.G., Longmore, A.J., Williams, P.M., Caldwell, J.A.R. 1983, MNRAS, **204**, 215

Elias, J. H., Frogel, J. A., Matthews, K., & Neugebauer, G. 1982, AJ, **87**, 1029

Gum, C.S. 1952, Observatory, **72**, 151

Lefloch, B., and Lazareff, B. 1994, A&A, **289**, 559

Luhman, K. 1999, ApJ, **525**, 466

Pettersson, B. 1984, A&A, **139**, 135

Reipurth, B. 1983, A&A, **117**, 183

Reipurth, B. and Pettersson, B. 1993. A&A **267**, 439.

Sahu, M., Pottasch, S.R., Sahu, K.C., Wesselius, P.R., Desai, J.N. 1988, A&A, **195**, 269

van Rensbergen , W., Vanbeveren, D., and de Loore, C. 1996, A&A, **305**, 825

Walter, F.M., Brown, A., Mathieu, R.D., Myers, P.C., & Vrba, F.J. 1988. AJ **96**, 297.

Walter, F.M. 2000 htp://www.ess.sunysb.edu/fwalter/CIRIM/cirim.html